ARTICLE

Three-Dimensional Cu-Ni Composite Superamphiphobic Surface via Electrodeposition and Fluorosilane Modification

Wei-yi Liu, Meng-fan Luo, Fang Luo, Yan Liu, Yan-zong Zhang*, Fei Shen, Xiao-hong Zhang, Gang Yang, Li-lin Wang, Shi-huai Deng

College of Environmental Sciences, Sichuan Agricultural University, Chengdu 611130, China

(Dated: Received on May 30, 2019; Accepted on August 30, 2019)

A superamphiphobic (SAP) surface was fabricated by electrodepositing Cu-Ni micro-nano particles on aluminum substrate and modifying via 1H,1H,2H,2H-perfluorodecyltrimethoxysilane. Scanning electron microscopy, X-ray diffraction, energy-dispersive X-ray spectroscopy, and Fourier-transform infrared spectroscopy were employed to investigate the morphology and chemical composition. The results showed that the SAP surface had three-dimensional micro-nano structures and exhibited a maximum water contact angle of 160.0°, oil contact angle of 151.6°, a minimum water slide angle of 0° and oil slide angle of 9°. The mechanical strength and chemical stability of the SAP surface were tested further. The experimental results showed that the SAP surface presented excellent resistance to wear, prominent acid-resistance and alkali-resistance, self-cleaning and anti-fouling properties.

Key words: Rough surface, Micro-nano structure, Low surface energy, Self-cleaning, Wear resistance, Chemical stability

I. INTRODUCTION

Enlightened by natural self-cleaning phenomena, such as lotus leaf and the wings of butterflies, superhydrophobic (SHP) coatings have been fabricated to protect metal surfaces from corrosive medium [1, 2]. While SHP surfaces rarely fulfill oleophobic demands in practical applications including oil transportation, daily cleaning, and so on. Therefore, superamphiphobic (SAP) surfaces become a specific need. Nevertheless, the preparation of SAP surfaces is very difficult because of its tiny nano-structures and low surface energy [3, 4].

Recently, several methods on the fabrication of SAP surface have been developed, including cycle-etching [5], laser processing [6], sol-gel processing [7], printing [8], electro-spraying technique [9], and electrodeposition [10, 11]. Among them, electrodeposition has been regarded as a promising method to construct SAP surface because of the advantages of being simple and easy to operate and control, low cost and also eco-friendly procedure. Different metal particles could form different microstructures of unique shapes during electrodeposition. For example, Zn [12], Ni [13], Cu [14] and Cr [15], *etc*, have been applied to electrodeposition, obtaining textures structures, cauliflower-like cluster binary structures, zigzag microstrips, and spongy morphology with multi nanopores, respectively. These rough structures facilitate the resulting surfaces to be superhydrophobic or even superamphiphobic according to the Wenzel or Cassiee-Baxter models [16, 17]. Bimetallic synergic effect is widely employed for catalysts [18], adsorbents [19], sensors [20], and so forth. Similarly, superhydrophobic or superoleophobic surface with two or more composite metals induces the formation of special structures, which can improve the surface mechanical strength and corrosion resistance [2, 21−23]. In addition, the presence of low surface energy components on the roughened surface can reduce the affinity of water to the surface [24−27]. It has been experimentally proven that the surface energy value for constituent groups in the descending order are CH_2 (36 J/m^2)>CH_3 (30 J/m^2)>CF_2 (23 J/m^2)>CF_3 (15 J/m^2) [27], and the surface chemistry modification of rough surfaces with a long-chain fluorocarbon is crucial in facilitating SAP property [28].

In this study, we provided an approach for fabricating a SAP Cu-Ni/FAS-17 composite surface on Al substrate. It was obtained by a simple electrodeposition process and then modified with FAS-17 (Scheme 1). Experiments were carried out to study the wettability of the SAP surface, as well as anti-abrasion, chemical stability, self-cleaning, and anti-corrosion properties.

II. EXPERIMENTS

A. Materials and reagents

The Al plates and copper plates (purity of 99.5%, thickness of 0.05 mm) were purchased from Re-

*Author to whom correspondence should be addressed. E-mail: yzzhang@sicau.edu.cn

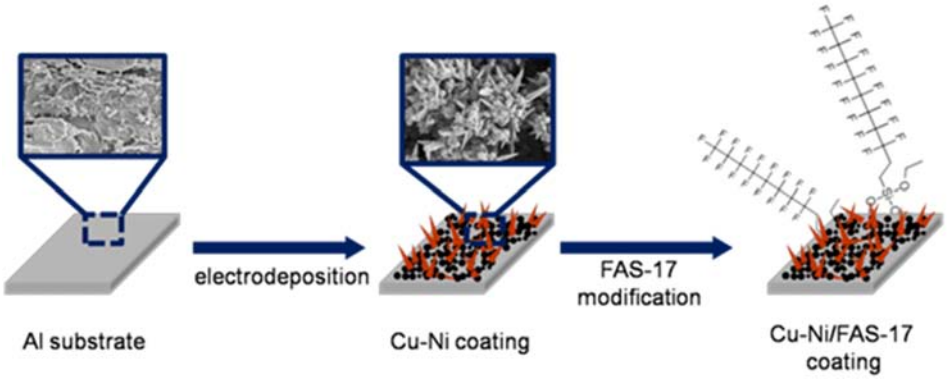

Scheme 1 Preparation process of Cu-Ni/FAS-17 coating.

search Institute of Northwest Nonferrous Metals of China. Hydrochloric acid (HCl, 36%−38%), ammonium hydroxide ($NH_3{\cdot}H_2O$, 25%−28%), anhydrous ethanol (C_3H_6O, 99.5%), sodium hypophosphite (NaH_2PO_2), sodium sulfate (Na_2SO_4), citriacidanhydrous ($C_6H_8O_7$), sodium dodecyl sulfate (SDS, $CH_3(CH_2)_{11}OSO_3Na$), nickel sulfate hexahydrate ($NiSO_4{\cdot}6H_2O$), copper(II) sulfate pentahydrate ($CuSO_4{\cdot}5H_2O$) were analytical pure grade and bought from Chengdu Kelon chemical reagent factory, China. 1H,1H,2H,2H-Perfluorodecyltrimethoxysilane (FAS-17, $C_{13}H_{13}F_{17}O_3Si$) was provided by the Nanjing Pinning Coupling Co., Ltd. Cooking oil was purchased from local store. Deionized water was used in all experiments.

B. Pretreatment of substrates

Aluminum and copper plates were cut into 35 mm× 52 mm×0.5 mm small pieces. The oxide film on the surface was removed by mechanical polishing with 800−1000 sandpaper, respectively. After washing with deionized water in sequence, the mixture was dried via a hair dryer and activated at 4 mol/L hydrochloric acid solution for 2 min at room temperature, followed by rinsing, drying and separation.

C. Fabrication of the SAP surface

The SAP Cu-Ni/FAS-17 composite coating was fabricated with the following processes. Al substrate and Cu plates were taken as cathode and anode in an electrolyte cell, respectively. The electrode spacing was fixed at 20 mm. $NiSO_4{\cdot}6H_2O$ (0.0625 mol/L), Na_2SO_4 (0.1 mol/L), $CuSO_4{\cdot}5H_2O$ (0.0625 mol/L), $C_6H_8O_7$ (0.05 mol/L), NaH_2PO_2 (0.025 mol/L) and SDS (0.12 g/L) were dissolved in distilled water, and used as electrolyte. The solution pH was adjusted to 5.5−6.0 with $NH_3{\cdot}H_2O$. The cathode specimens were removed from the solution, followed by washing and drying with hair dryer after electrodepositing process at room temperature. Next, the Cu-Ni composite coating samples were immersed in 1.0 wt% fluoroalkylsilane-ethanol solution for 2 h at room temperature. Then, the samples were taken out, adequately cleaned and dried by hair dryer. Finally, a Cu-Ni/FAS-17 composite coated with a micro-nano structure on Al substrate was obtained, which was labeled as SAP surface.

D. Characterization

The surface wettability was measured by water contact angles (WCAs), oil contact angles (OCAs), water slide angles (WSAs) and oil slide angles (OSAs) using a contact-angle meter (JC2000C2, Shanghai Zhongjin Instrument Co., Ltd.) at room temperature. The surface morphology was observed by scanning electron microscopy (SEM, S-4800, accelerating voltage 20 kV, Hitachi, Japan). The crystal structure of the coating was examined using X-ray diffractometer (XRD, Bruker-AXS: D8 Advance, Germany). The chemical bonds were analyzed through Fourier transform infrared spectroscopy (FTIR, Magna-IR 750, Nicolet, USA). The surface chemical composition was measured by using X-ray photoelectron spectroscopy (XPS, K-Alpha, Thermo Scientific, USA) and energy dispersive spectrometer (EDS, 7593-H, HORIBA, Japan).

The wear-resistant ability of the SAP surface was characterized via an abrasion test. A rough cleaning cloth was used as an abrasion surface. The SAP surface was placed on the cleaning cloth with weight of 500 g, and then pulled in one direction at speed of 5 mm/s. The corrosion resistance was investigated by immersion test in the 3.5 wt% NaCl solution for 15 days at speed of 1500 r/min. The chemical stability was analyzed by soaking the SAP samples in solution with different pH values for 4 h. The pH was adjusted by HCl or NaOH solution. The self-cleaning test was performed by putting the samples into the stirred artificial polluted solution for 1 min at speed of 700 r/min, which was comprised of 200 g oil, 200 g cement, 200 g talc powder and 400 mL water.

DOI:10.1063/1674-0068/cjcp1905109

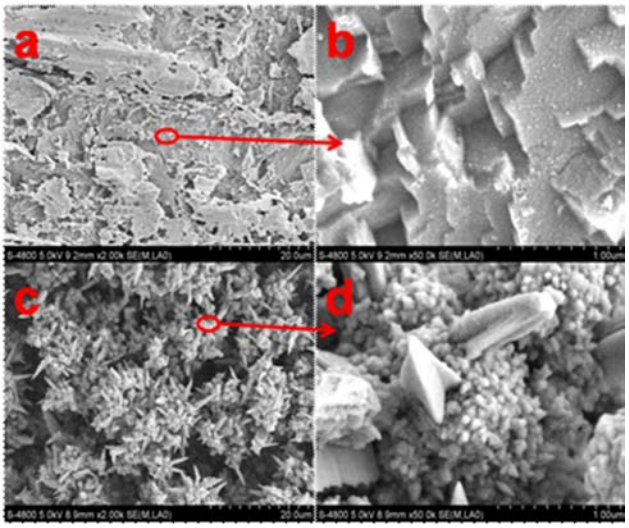

FIG. 1 SEM images of (a) polished aluminum and (c) SAP surface, (b) and (d) partial enlarged view of the marked region in (a) and (c).

III. RESULTS AND DISCUSSION

A. Surface morphology

The Al surfaces became uneven after polishing and activating (FIG. 1(a)), and a ladder-like structure could be observed (FIG. 1(b)). However, the SAP surface (Cu-Ni/FAS-17 composite coating) was covered with many cauliflower-like and thorn-like micro-nano structures (FIG. 1(c)). Obviously, the three-dimensional cauliflower-like and thorn-like micro-nano structures were distributed unevenly on the Al substrate. It was further discovered that the micro-nano structures consisted of agglomerated nano-particles (FIG. 1(d)). Meanwhile, sharp protuberances grew out of the aggregated structures. The rough structures on SAP surface could form a composite solid-liquid-air interface. The Laplace pressure force was directed upward when the droplets were placed on the surface, which can effectively prevent the liquids from penetrating into the textures [29−31].

B. Chemical composition and crystalline structure

For Al substrate, four diffraction peaks at 38.3°, 44.7°, 64.9°, and 78.5° are respectively assigned to the crystal faces of Al(111), Al(200), Al(220), and Al(311) (PDF No.85-1327) (FIG. 2a(i)). For the SAP surface, four new characteristic peaks appear at 43.3°, 50.4°, 74.2°, and 76.0° (FIG. 2a(ii)), corresponding to the crystal faces of Cu(111) (PDF No.04-0836), Cu(200), Cu(220), and Ni(220) (PDF No.45-1027), respectively. Additionally, two adjacent peaks at 44.7° and 44.5° are ascribed to Al(220) (PDF No.85-1327) and Ni(111) (PDF No.45-1027), which might overlap in FIG. 2a(ii).

It can be observed that the existence of Al, Mg, and O elements in Al substrate, as shown in FIG. 2b(i). The elements of Ni, Cu and C, O, F could be further found in the Cu-Ni/FAS-17 composite coating (FIG. 2b(ii)). The Cu and Ni elements are determined from the $CuSO_4$ and $NiSO_4$, while C, O and F elements originate from FAS-17 in the Cu-Ni/FAS-17 coating. Moreover, strong peaks of Cu 2p, Ni 2p, F 1p, O 1s and C 1s on SAP surface appear at 932.2, 852.8, 688.9, 531.3, and 284.8 eV, respectively [13, 32] (FIG. 2(c)). It is in agreement with the EDS analysis.

The binding energies of Cu 2p and Ni 2p demonstrate the presence of metallic Cu and Ni in the Cu-Ni/FAS-17 composite coating [33]. It is also proven that the porous layers (FIG. 1) are entirely metallic state [34]. Compared with the FT-IR spectrum of Cu-Ni coating, the SAP surface displays obvious differences (FIG. 2(d)). The -CF_3 and -CF_2 stretching vibration peaks are observed at 1245.3, 1205.4, and 1145.2 cm^{-1}. Si−O stretching vibration peaks appear at 1065.9, 1046.8, and 983.8 cm^{-1}, respectively [35]. The results indicate that the surface is coated by FAS-17.

C. Wettability of sample surface

In FIG. 3(a), WCA and OCA increased with the deposition time extending within 15 min, and CA was the max when deposition time was 15 min. The insert of FIG. 3(a) shows good superamphiphobicity that was obtained on the surface with deposition time of 15 min. FIG. 3(b) shows the surface morphology at deposition time of 8 min, which is flatter than FIG. 1(c). This is attributed to that the micro/nano structures developed gradually on the surface as time went on. With the extension of the deposition time to 25 min, the WCA and OCA decreased to 129.0° and 117.1°, respectively.

In addition, WCA and OCA of Al substrate were 73.4° and 22.1°, respectively, while they increased to 145.5° and 84.4° after being modified with FAS-17 (FIG. 3(c)). Once the Cu-Ni coating was electrodeposited on Al substrate, WCA and OCA reached 158.4° and 112.4°, which were higher than those of Al/FAS-17. FIG. 3(d) shows CAs and SAs of different liquid drops on SAP surface, which were almost above 150° and below 10°, respectively, except lubricating oil and diesel oil. The difference of CAs and SAs was mainly caused by the viscosity difference of oils. These results indicate that low surface energy molecules and the rough micro-nano structures are both able to enhance the hydrophobicity and oleophobicity of the solid surfaces. Especially the rough micro-nano structures are more effective than low surface energy molecules. The micro-nano structures can effectively capture air, thus prevent water/oil droplets and surface in contact. After the Cu-Ni coating was modified by FAS-17, WCA and OCA of SAP surface reached higher up to 160.0° and 151.6°. The result reveals that the rough micro-nano structures with low surface energy groups display a synergistic effect

DOI:10.1063/1674-0068/cjcp1905109

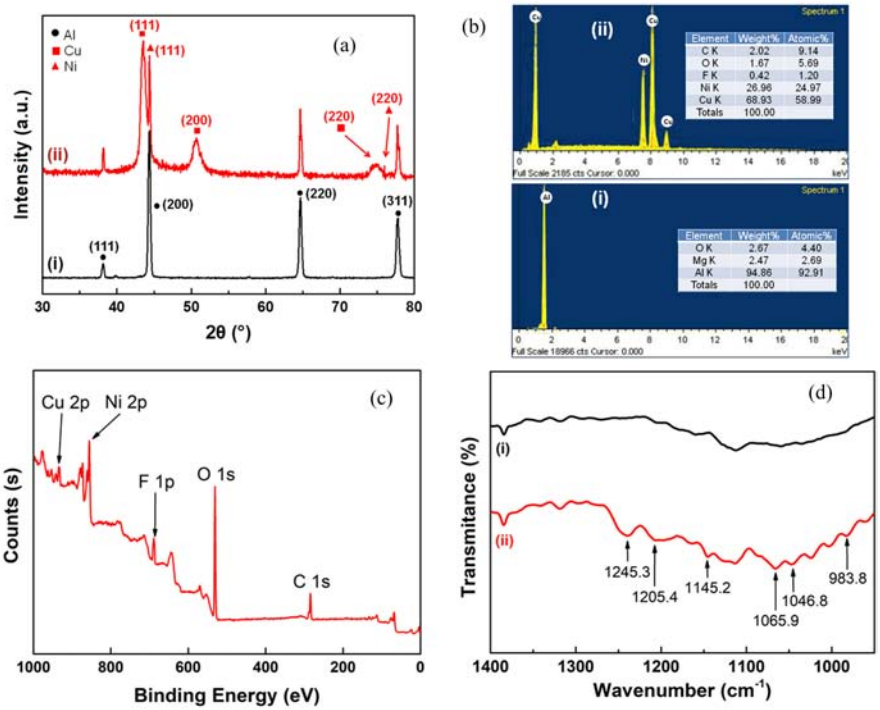

FIG. 2 (a) XRD patterns of (i) Al substrate and (ii) SAP surface, (b) EDS spectra, (c) XPS spectrum of Al substrate and SAP surface, and (d) FT-IR spectra of (i) Cu-Ni and (ii) SAP surface.

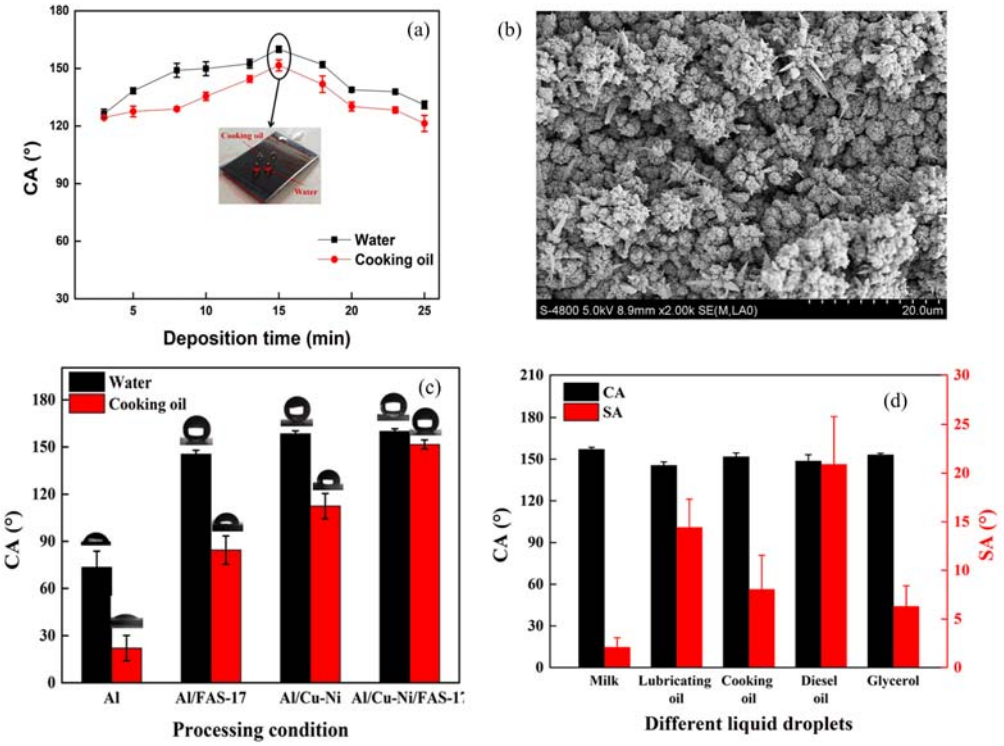

FIG. 3 (a) WCAs and OCAs with different deposition time. (b) SEM image of surface deposition for 8 min. (c) WCAs and OCAs under different processing conditions. (d) Optical image of water and cooking oil droplets on SAP surface.

DOI:10.1063/1674-0068/cjcp1905109

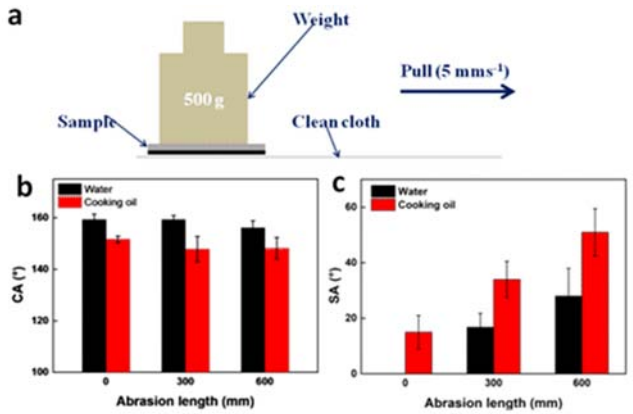

FIG. 4 (a) The methodology of the abrasion test. (b) WCAs and OCAs, (c) WSAs and OSAs during abrasion test.

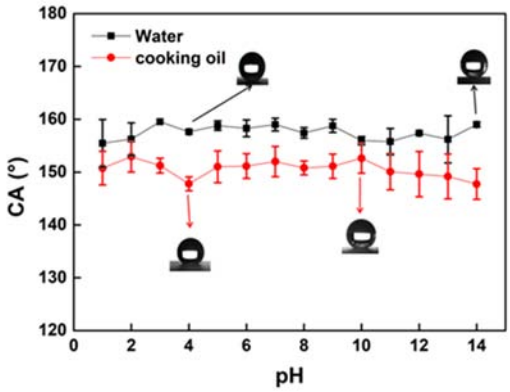

FIG. 5 Effect of pH value in solution on the wettability of the SAP surface.

and show superior hydrophobicity and oleophobicity.

D. Properties of SAP surface

1. Mechanical and chemical stability

FIG. 4(a) shows the methodology of the abrasion test. WCA of the SAP surface still remained above 155° even after abrasion length of 600 mm, and the OCAs slightly decreased to 148.2° (FIG. 4(b)). WSA and OSA increased to 28° and 51° (FIG. 4(c)), respectively, which meant superhydrophobicity was damaged by mechanical abrasion. The SAP surface exhibited excellent resistance to wear, which was more improved as compared to the reported superhydrophobic coatings [11]. The wear resistance, as well as the mechanical stability of SAP surface could be attributed to the enhanced roughness from the three-dimensional micro-nano structures.

WCAs and OCAs exceed 155.4° and 147.7° respectively, even at pH=1 and pH=14 (FIG. 5). It exhibits that the SAP surface owns satisfactory acid-resistance and alkali-resistance. It also illustrates that SAP surface can effectively protect the Al surface. This could be the reason that there are 68.9 wt% Cu elements (FIG. 2b(ii)) which do not react with diluted acid and alkali solution.

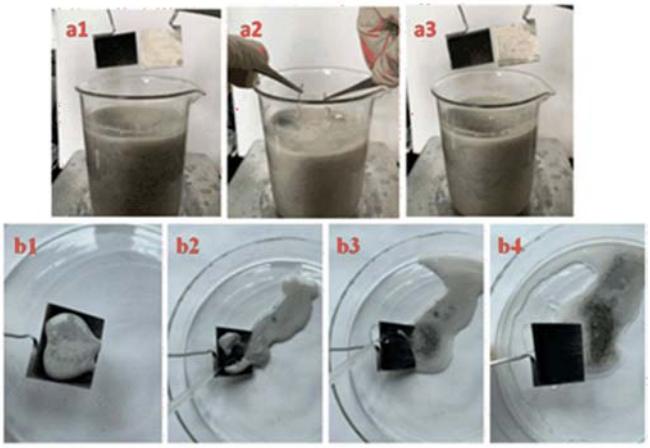

FIG. 6 Self-cleaning effect experiments: (a1, a2, a3) SAP surface immersed into the contaminated water, (b1) SAP surface dusted with cement paste, (b2, b3) SAP surface cleaned with distilled water, (b4) cement paste completely removed from the surface.

The anti-corrosive property of SAP surface was also examined in the 3.5 wt% NaCl solution under stirring condition for 15 days. The result shows that WCAs were 161.54° and 159.77° before and after test, respectively, and OCA dropped from 152.92° to 147.01°. The flowing brine is more corrosive than the static brine, nevertheless, SAP surface also maintains the prominent anti-corrosive property.

2. Self-cleaning and anti-fouling property

In FIG. 6 (a1, a2, and a3), the SAP surface and Al substrate were immersed into the contaminated water with the stirring rate of 700 r/min for 1 min. The SAP surface still maintained clean and the Al substrate was covered with pollutant. Further, when the pollutant was dropped on the SAP surface, all the pollutant was easily washed away by water and the SAP surface was as clean as before (FIG. 6 (b1, b2, b3, and b4)). The excellent self-cleaning property was the combined effects of the rough micro-nano structures and low surface energy materials. The massive amounts of air were filled with rough micro-nano structures, restraining the contact of the pollutants with surface efficiently. Meanwhile, the modification of FAS-17 decreased the surface energy of the SAP surface, which further prevented the penetration of liquid into the coating.

IV. CONCLUSION

A simple and high efficiency approach for the preparation of the superamphiphobic surface on aluminum

DOI:10.1063/1674-0068/cjcp1905109

substrate was provided. Electrodeposition and modification display a synergistic effect on promoting superamphiphobic properties. The superamphiphobic surface possesses not only excellent resistance to wear, but also prominent acid-resistance and alkali-resistance, self-cleaning and anti-fouling properties. The fabrication process is adjustable with parameters and reliable on repeatability, which makes it suitable for not only aluminum substrate, but also other metal substrates.

V. ACKNOWLEDGMENTS

This work was supported by Science and Technology Department of Sichuan Province (2017JZ0021, 2017SZ0039), Education Department of Sichuan Province (17ZA0298) and Innovative Training Program for College Students of Sichuan Province (No.201810626118).

[1] Y. Liu, J. Z. Xue, D. Luo, H. Y. Wang, X. Gong, Z. W. Han, and L. Q. Ren, J. Colloid Interface Sci. **491**, 313 (2017).
[2] Q. Y. Yu, Z. X. Zeng, W. J. Zhao, M. H. Li, X. D. Wu, and Q. J. Xue, Colloids Surf. A **427**, 1 (2013).
[3] R. V. Lakshmi, P. Bera, C. Anandan, and B. J. Basu, Appl. Surf. Sci. **320**, 780 (2014).
[4] H. Li and S. R. Yu, J. Taiwan Inst. Chem. E. **63**, 411 (2016).
[5] N. Wen, S. Peng, X. J. Yang, M. Y. Long, W. S. Deng, G. Y. Chen, J. Q. Chen, and W. L. Deng, Adv. Eng. Mater. **19**, 1600879 (2017).
[6] Y. X. Song, C. Wang, X. R. Dong, K. Yin, F. Zhang, Z. Xie, D. K. Chu, and J. A. Duan, Opt. Laser Technol. **102**, 25 (2018).
[7] B. B. Xia, H. T. Liu, Y. N. Fan, W. Zhu, and C. Geng, Adv. Eng. Mater. **19**, 1600572 (2017).
[8] H. X. Wang, Y. H. Xue, and T. Lin, Soft Matter **7**, 8158 (2011).
[9] K. N. Al-Milaji and H. Zhao, Appl. Surf. Sci. **396**, 955 (2017).
[10] G. He, S. X. Lu, W. G. Xu, P. Ye, G. X. Liu, H. T. Wang, and T. L. Dai, J. Alloys Compd. **747**, 772 (2018).
[11] H. Y. Wang, Y. X. Zhu, Z. Y. Hu, X. G. Zhang, S. Q. Wu, R. Wang, and Y. J. Zhu, Chem. Eng. J. **303**, 37 (2016).
[12] B. Y. Zhang, S. X. Lu, W. G. Xu, and Y. Y. Cheng, Appl. Surf. Sci. **360**, 904 (2016).
[13] Y. Liu, S. Y. Li, Y. M. Wang, H. Y. Wang, K. Gao, Z. W. Han, and L. Q. Ren, J. Colloid Interface Sci. **478**, 164 (2016).
[14] L. J. Liu, W. K. Liu, R. F. Chen, X. Li, and X. J. Xie, Chem. Eng. J. **281**, 804 (2015).
[15] B. Zhang, H. T. Feng, F. Lin, Y. B. Wang, L. P. Wang, Y. P. Dong, and W. Li, Appl. Surf. Sci. **378**, 388 (2016).
[16] A. B. D. Cassie and S. Baxter, Trans. Faraday Soc. **40**, 546 (1944).
[17] R. N. Wenzel, Ind. Eng. Chem. **28**, 988 (1936).
[18] D. Wang, A. Villa, F. Porta, L. Prati, and D. S. Su, J. Phys. Chem. C **112**, 8617 (2008).
[19] L. L. Zhao, Y. Huang, H. Y. Chen, Y. X. Zhao, and T. C. Xiao, Fuel **197**, 20 (2017).
[20] F. Amiripour, S. N. Azizi, and S. Ghasemi, Biosens. Bioelectron. **107**, 111 (2018).
[21] H. B. Lee, Tribol. Lett. **50**, 407 (2013).
[22] J. L. Song, S. Huang, K. Hu, Y. Lu, X. Liu, and W. J. Xu, J. Mater. Chem. A **1**, 14783 (2013).
[23] Y. F. Zhou, T. Hang, F. Li, and M. Li, Appl. Surf. Sci. **271**, 369 (2013).
[24] J. D. Brassard, D. K. Sarkar, and J. Perron, Appl. Sci. **2**, 453 (2012).
[25] X. J. Guo, C. H. Xue, S. T. Jia, and J. Z. Ma, Chem. Eng. J. **320**, 330 (2017).
[26] Y. Q. Qing, C. N. Yang, Q. Q. Zhao, C. B. Hu, and C. S. Liu, J. Alloys Compd. **695**, 1878 (2017).
[27] Z. S. Saifaldeen, K. R. Khedir, M. T. Camci, A. Ucar, S. Suzer, and T. Karabacak, Appl. Surf. Sci. **379**, 55 (2016).
[28] J. Tsibouklis and T. G. Nevell, Adv. Mater. **15**, 647 (2003).
[29] F. Z. Chen, J. L. Song, Y. Lu, S. Huang, X. Liu, J. Sun, C. J. Carmalt, I. P. Parkinb, and W. J. Xu, J. Mater. Chem. A **3**, 20999 (2015).
[30] C. D. Jin, J. P. Li, S. J. Han, J. Wang, and Q. F. Sun, Appl. Surf. Sci. **320**, 322 (2014).
[31] Y. Liu, H. J. Cao, S. G. Chen, and D. A. Wang, J. Phys. Chem. C **119**, 25449 (2015).
[32] Q. Y. Wen, F. Guo, Y. B. Peng, and Z. G. Guo, Colloids Surf. A: Physicochem. Eng. Aspects **539**, 11 (2018).
[33] A. L. Ma, S. L. Jiang, Y. G. Zheng, and W. Ke, Corros. Sci. **91**, 245 (2015).
[34] J. Zhang, M. D. Baro, E. Pellicer, and J. Sort, Nanoscale **6**, 12490 (2014).
[35] E. J. Lee, A. K. An, T. He, Y. C. Woo, and H. K. Shon, J. Membr. Sci. **520**, 145 (2016).

DOI:10.1063/1674-0068/cjcp1905109